

Research Article

Theme: *Quality by Design: Case Studies and Scientific Foundations*

Guest Editors: *Robin Bogner, James Drennen, Mansoor Khan, Cynthia Oksanen, and Gintaras Reklaitis*

Quality-by-Design III: Application of Near-Infrared Spectroscopy to Monitor Roller Compaction In-process and Product Quality Attributes of Immediate Release Tablets

Ravikanth Kona,¹ Raafat M. Fahmy,² Gregg Claycamp,² James E. Polli,¹ Marilyn Martinez,² and Stephen W. Hoag^{1,3}

Received 9 September 2013; accepted 15 July 2014; published online 16 October 2014

Abstract. The objective of this study is to use near-infrared spectroscopy (NIRS) coupled with multivariate chemometric models to monitor granule and tablet quality attributes in the formulation development and manufacturing of ciprofloxacin hydrochloride (CIP) immediate release tablets. Critical roller compaction process parameters, compression force (CF_i), and formulation variables identified from our earlier studies were evaluated in more detail. Multivariate principal component analysis (PCA) and partial least square (PLS) models were developed during the development stage and used as a control tool to predict the quality of granules and tablets. Validated models were used to monitor and control batches manufactured at different sites to assess their robustness to change. The results showed that roll pressure (RP) and CF_i played a critical role in the quality of the granules and the finished product within the range tested. Replacing binder source did not statistically influence the quality attributes of the granules and tablets. However, lubricant type has significantly impacted the granule size. Blend uniformity, crushing force, disintegration time during the manufacturing was predicted using validated PLS regression models with acceptable standard error of prediction (SEP) values, whereas the models resulted in higher SEP for batches obtained from different manufacturing site. From this study, we were able to identify critical factors which could impact the quality attributes of the CIP IR tablets. In summary, we demonstrated the ability of near-infrared spectroscopy coupled with chemometrics as a powerful tool to monitor critical quality attributes (CQA) identified during formulation development.

KEY WORDS: chemometrics; crushing force; disintegration; near-infrared spectroscopy; partial least square; principal component analysis; quality by design; roller compaction.

INTRODUCTION

Recently, dry granulation using roller compaction (RC) has grown in popularity, as the process is economical, energy efficient, easily automated, and suitable for drugs that are sensitive to heat and moisture (1). In roller compaction, the powder blend is compressed and compacted between two counter-rotating rollers resulting in ribbon which when milled produces granules of desired size. Despite its apparent simplicity, it is quite challenging to understand the influence of RC process variables on the critical quality attributes (CQA) of a dosage form. Process parameters such as roll pressure (RP), feed screw speed (FSS), and roll speed (RP) were known to be critical and could impact process feasibility, compaction properties of the ribbons, and the tableability of

granules (1). It is known that increasing in the FSS (at constant roll speed and roll gap) leads to the densification of the ribbon resulting in caking of material thereby interrupting the flow of the powder between the rollers. Operating at low FSS could result in poor-quality ribbon with low density due to insufficient powder at the nip-zone region. Roll speed was found to influence the dwell time of the powder; this is critical for a plastically deforming materials such as microcrystalline cellulose (MCC) where low roll speeds increase the dwell time and result in loss of compactability leading to tablets with lower hardness and friability (2,3). In case of materials that exhibit significant elastic recovery, higher roll speed may lead to cracking, resulting in poor-quality ribbon due to a shorter dwell time (4,5). Higher RP on the other hand was found to increase the density of the ribbon and in turn produces tablets with higher crushing force (CF) and low friability (6,7). Roller surfaces (smooth vs knurled) were shown to influence the bulk and tapped densities of the granules (8).

In addition to process parameters, material properties such as morphology and the particles size of excipients were found to influence the ribbon quality, granule size distribution, content uniformity, flowability, and the compaction properties

¹School of Pharmacy, University of Maryland, 20 N. Pine Street, Baltimore, Maryland 21201, USA.

²Office of New Animal Drug Evaluation, Center for Veterinary Medicine, FDA, Rockville, Maryland 20855, USA.

³To whom correspondence should be addressed. (e-mail: shoag@rx.umaryland.edu)

of the resulting tablets (6). Therefore, it is critical to identify the sources of variability arising both from process and input materials and develop a reliable and well-understood process that will consistently ensure a pre-defined quality at the end of the manufacturing process. A process is considered well understood and controlled when all the sources of variability that affect product quality are identified, monitored, and controlled. This can be achieved through the proper design and analysis of critical process and material attributes that influence the quality of a dosage form (9). To establish process control, it is critical to describe and justify how in-process controls and the control of input materials (drug substance and excipients) and intermediates (in-process materials) contribute to the final product quality. A primary goal of establishing a control strategy is to shift the control of attributes upstream in the manufacturing process and minimize the need for end-point quality testing (ICH Q8) (10).

The conventional method of quality testing of pharmaceutical products often involves sampling the product in a batch process and performing laboratory QC tests. Today, with the availability of newer technologies, significant opportunities exist for real-time testing in product development, manufacturing, and the quality testing of products. This shift in the process control philosophy from a conventional end-phase testing to a continuous, or nearly so, in-line systems of quality testing is designed to build quality into the system thereby avoiding the lag time associated with the offline techniques. One such monitoring tool is near-infrared spectroscopy (NIRS). Some advantages of NIR over other spectroscopy tools include rapid, nondestructive, and minimal sample preparation (9,11–13). In the last decade, there are several articles published on the use of NIRS as process analytical technology (PAT) tool for roller compaction. Gupta *et al.* used slope of best-fit line through a near-infrared spectra's baseline to quantify the strength of ribbons; strength was determined using a three-point beam-bending test (14). They also demonstrated the use of NIRS to determine in real-time compact tensile strength, young's modulus and particle size during roller compaction (15). Soh *et al.* used roll gap and NIR spectral slope in combination with roller compaction process parameters to predict roller compaction responses. By evaluating these two variables, the authors were able to assess the influence of raw material properties on the roller compaction process (16). Although there are several articles on application on application NIRS in roller compaction, little attention was paid to the material attributes such as excipient grades and source variability on the final quality, which is critical in formulation development under quality-by-design (QbD) paradigm. Currently, there is limited literature available where risk factors that could potentially impact the quality target product profiles (QTPP) were systematically identified and monitored using NIRS.

Figure 1 shows the main product development steps outlined in the ICH guidance Q8 (R^2), Q9, and Q10 (10,17,18). In our previous studies, we examined steps 1, 2, and 3; *i.e.*, defining target product profiles and identify CQAs (19). Steps 1 and 2 were studied in the first manuscript (10). Next, the authors examined the use of quantitative risk models to assess the risk and define the design space (20). The objective of this paper is to study critical factors identified

from our earlier studies in more detail to gain better process understanding and use NIR spectroscopy coupled with multivariate chemometric models (principal component analysis (PCA) and partial least squares (PLS)) to monitor the product quality attributes that were identified from our earlier studies in order to establish process control strategy.

The first part of this paper focuses on the characterization of the granules and tablets obtained using various processing parameters. Here, critical formulation variables such as binder source and lubricant type that were identified in the authors' previous studies were further evaluated (18). HPC-Klucel® EXF and HPC-L binder grades were selected based on the previous studies performed by Desai *et al.* In these studies, both HPC grades meet the NF criteria and exhibit no significant differences in the average molecular weight; but they were found to influence the dissolution rate of hydrochlorothiazide (21). For lubricants, Mg stearate monohydrate (MgSt-M) and dihydrate (MgSt-D) forms were evaluated. The 2nd part of this paper focuses on developing multivariate chemometric models to quantify granules size and develop PLS calibration models to predict CQAs, such as tablet CF and disintegration times (DTs). The third part of this paper focuses on application of validated model to external batches manufacture at different locations. In this study, ciprofloxacin hydrochloride (CIP) monohydrate was used as a model drug (Fig. 2), which belongs to Biological Classification System (BCS) Class II (poor soluble and high permeable) (22).

MATERIALS AND METHODS

Materials

CIP monohydrate (lot no. CI06026) was obtained from R.J. Chemicals, Coral Springs, FL (Quinica Sintetica, Madrid, Spain). MCC, Avicel® PH-102 (lots no. P208820014 and P209820744) was donated by FMC Biopolymer (Newark, DE); hydroxypropyl cellulose (HPC), Klucel® EXF (lots no. 99768 and 99769) was generously gifted by Hercules Incorporation (Hopewell, VA); and HPC-L (lot no. NHG-5111) was obtained from Nisso America Inc. (New York, NY). Starch 1500® (lots no. IN502268 and IN515968) was generously donated by Colorcon (Indianapolis, IN). Magnesium stearate monohydrate (lot no. MO5676) and magnesium stearate dihydrate (lot no. JO3970) was obtained from Covidien (Hazelwood, MO).

Design of Experiments

Table I shows the base CIP formulation used in this study; the formulation development and the identification of the CQA is described in our previous study (19). Table II shows the factors studied and the design employed. Two binder types, hydroxypropyl cellulose (Klucel® EXF and Nisso®-L) and two lubricant types, magnesium stearate (MgSt-M and MgSt-D) are the formulation variables evaluated. Three RPs (20, 80, and 140 bar) and three compression force (8, 12, and 16 kN) were studied as processing parameters. In addition, binder and disintegrant levels were evaluated leading to total of 42 different lots. Batches 15–25 were manufactured at different site from batches 1 – 14, from now on batches 15–25 will be referred to as manufacturing site 2 batches. At site 2,

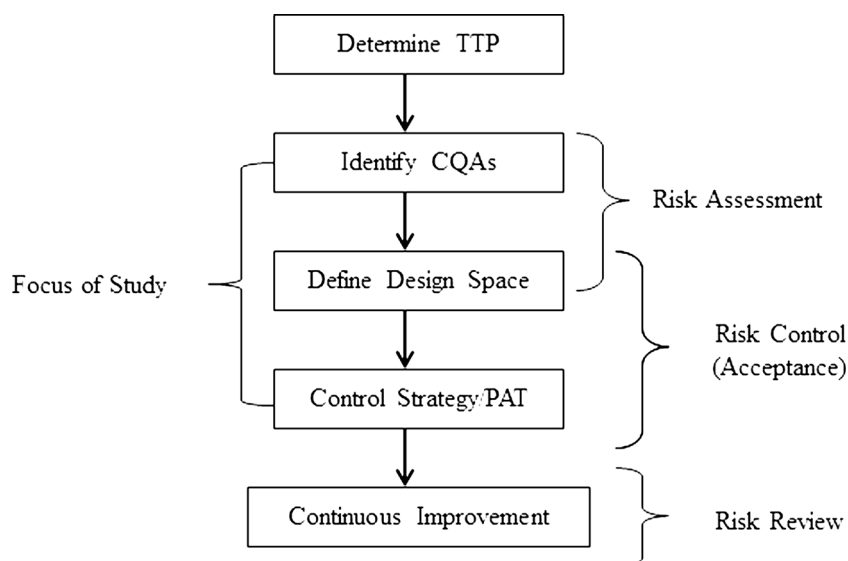


Fig. 1. QbD drug product development flow chart showing principal steps

roller compaction was carried out on an identical model roller compactor, granulation was carried out at the same RP, FSS/RP ratios, binder, and disintegrant levels as site 1, see Table II, batches 15–25.

NIR Measurements and Spectral Analysis

A rapid content analyzer (RCA) DS 6500 spectrometer (FOSS NIRsystems, Inc., Laurel, MD) was used to scan the samples from 400 to 2,500 nm, and the final spectrum was the average of 32 scans. The powder blends and granules were scanned in glass scintillation vials; the tablets were scanned directly without any container; all samples were scanned in diffuse reflectance mode; these samples were considered to be at-line sample measurements. The NIR models were developed using Vision® version 3.2 software. The PCA score plots were obtained from MatLab 7.0.4 (The MathWorks Inc. Natick, MA) with PLS Toolbox 3.0 software (Eigenvector Research, Inc., Manson, WA). To compare the laboratory data and model predictions, calculated from the at-line spectra, a paired *t* test was performed and *p* values <0.05 were considered significant. ANOVA was performed to study the influence of both formulation and processing variables on the characteristics of granules and tablets. Critical *p* values <0.05 were considered significant. Table III is the summary of regression coefficients (*b*) and probability (*p*) values from linear

regression of the responses studied. The sign for coefficients indicate the direction of the relationship where a positive sign indicate direct and a negative sign indicates inverse relationship.

Granule Production Via Roller Compaction

Figure 3 illustrates the flow chart for the manufacture of CIP immediate release tablets using roller compaction. Physical mixtures of CIP, Avicel® PH-102, Klucel®, Starch 1500®, and MgSt were mixed in a 2- or 16-qt V-blender (Patterson Kelly, Co, East Stroudsburg, PA) without intensifier bar rotating at 30 rpm for 1 kg batches 15–25 and 3.6 kg batches 1–14, respectively. The blends were compacted on a roller compactor (Alexanderwrek® W120, Horsham, PA) equipped with rollers (25 mm diameter) having a knurled surface. The processing parameters are described in Table II. For all batches, the mill impeller speed was maintained at 50 rpm. The ribbons were milled in two stages (coarse and fine) using mesh sizes 10 and 16, respectively. The extragranular portion which consists of Starch 1500® and Magnesium stearate was added and mixed with the roller compacted granules; this blend was mixed in the same V-blender

Table I. Base Formulation for CIP Immediate Release Tablets; Note for All Batches, the Disintegrant Was Always Added 50% Intragranular and 50% ExtraGranular

	Percent (w/w)
Intragranular portion	
CIP	50
Microcrystalline cellulose (Avicel® PH-102)	37
Hydroxypropyl cellulose	2
Starch® 1500	5
Magnesium stearate	0.5
Extragranular portion	
Starch® 1500	5
Magnesium stearate	0.5
Total	100

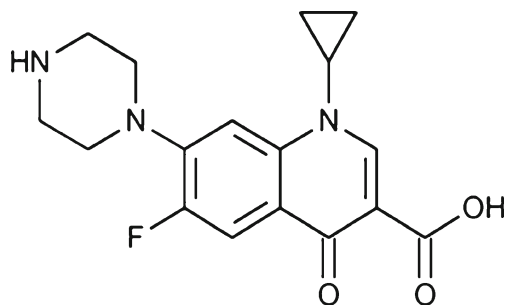


Fig. 2. Ciprofloxacin chemical structure

Table II. Formulation and Process Variables Studied for CIP Immediate Release Formulation Development and for NIR Calibration Model Development; Granule and Tablet Experimental Results Measured as Described in the Experimental Section

Batches ^a	RP	FSS/RP ratio	HPC (source)	MgSt (type)	EXF (%; w/w)	Starch (%; w/w)	Average granule d (μm)±STD	Span (μm)±STD	CF ^b (kp)±STD	DT ^c (min)±STD
1	20	5	+	+	2	10	98.9±13.4	6.6±2.9	15.5±0.5	4.0±0.9
2	80	5	+	+	2	10	160.7±9.3	7.1±2.2	9.3±0.5	8.5±1.4
3	140	5	+	+	2	10	183.5±2.3	5.3±0.5	6.8±0.6	13.2±2.5
4	20	5	–	+	2	10	89.1±10	6.8±1.9	15.3±0.6	3.5±0.5
5	80	5	–	+	2	10	161.5±6.8	5.6±0.9	9.7±0.8	8.0±2.2
6	140	5	–	+	2	10	193.4±9.6	4.4±0.7	6.6±0.6	15.5±1.9
7	20	5	–	–	2	10	90.2±5.0	5.0±0.8	16.5±1.0	3.5±0.8
8	80	5	–	–	2	10	173.7±3.4	4.9±0.1	9.0±0.6	7.7±1.0
9	140	5	–	–	2	10	210.9±5.2	3.9±0.4	6.8±0.8	11.7±2.5
10	20	5	+	–	2	10	95.5±3.5	4.8±0.1	14.6±1.3	3.2±0.4
11	80	5	+	–	2	10	179.8±8.4	4.6±0.1	10.5±0.8	7.7±1.6
12	140	5	+	–	2	10	231.7±5.7	3.5±0.2	7.2±0.8	16.3±0.7
13	80	5	+	+	4	10	149.0±9.4	5.5±0.4	9.1±0.9	28.0±7.5
14	80	5	+	+	4	14	151.3±14.4	5.7±1.9	9.1±1.0	21.7±0.8
15	80	5	+	+	2	10	147.9±7.2	18.3±5.5	4.0±0.8	7.7±4.5
16	80	7	+	+	2	10	254.0±18.4	3.4±0.3	3.3±0.6	4.7±1.2
17	80	3	+	–	2	10	152.8±4.2	6.8±1.0	6.3±0.8	1.0±0
18	140	7	+	–	2	10	298.4±26.6	2.8±0.3	2.2±0.4	6.3±2.9
19	140	5	+	–	2	10	333.9±29.9	2.3±0.3	3.6±0.3	4.3±1.2
20	140	5	+	+	2	10	140.0±13.6	16.5±6.0	3.7±0.6	2.7±0.6
21	140	3	+	+	2	10	263.0±33.3	3.9±0.3	5.3±0.6	2.7±0.6
22	80	5	+	+	4	10	154.6±26.4	18.6±10.8	5.5±0.7	21.0±6.2
23	80	5	+	+	4	10	154.6±26.4	18.6±10.8	6.5±0.7	36.3±6.7
24	80	5	–	+	6	8	157.3±29.0	12.7±7.0	5.0±1.4	45.7±7.2
25	80	5	–	–	3	10	251.5±8.2	4.0±0.4	4.6±0.4	42.0±4.4

HPC source, Klucel® EXF (+) and Nisso-L (–); magnesium stearate type, MgSt-M (+) and MgSt-D (–); average granule volume mean diameter D(4,3), and span which is the width of the distribution as described by 10%, 50%, and 90% quantiles and are average of three runs; crushing force (CF) and disintegration time (DT) are average of six tablets; the batches 1–14 were compressed to a 8-, 12-, and 16-kN peak compression force leading to 42 batches. Batches 15–25 were only compressed to a 12-kN peak compression force. In this table, only the data for the 12-kN peak compression force are shown; see text and figures for discussion of the 8- and 16-kN results

^a Average of three runs

^b Average of six tablets

^c Average of five tablets

for an additional 3 min. Approximately 2 g samples were collected before and after RC for the NIR scans, see next section for details. For site 2, same model RC fitted with identical rollers, fine, and coarse mesh was used to manufacture granules. For processing conditions, refer Table II (batches 15–25).

Blend Uniformity Study

Prior to granulation, blend uniformity was assessed for all lots using NIR and a PLS model. The blend uniformity

calibration model was built using 27 offline calibration samples comprising nine different concentrations of ciprofloxacin ranging from 45% to 61%, see Table IV. The CIP concentration was adjusted with MCC. For each calibration sample, a total of 10 g was prepared for each concentration studied, see Table IV. The samples were blending in a Turbula® mixer (Glen Mills Inc., Clifton, NJ) for 7 min. The blend was divided into *ca* 2 g aliquots and transferred into borosilicate glass scintillation vials with screw cap (VWR®, model no. 66021646) for NIR scanning. To assess blend uniformity,

Table III. Summary of Regression Coefficients (*b*) and *p* Values for Granules and Tablets for Batches 1–14

Variables	Granule size (μm)		CF (kp)		DT (min)		Q30	
	<i>b</i>	<i>p</i> value	<i>b</i>	<i>p</i> value	<i>b</i>	<i>p</i> value	<i>b</i>	<i>p</i> value
Intercept	183.7	–	7.44	–	17.08	–	84.65	–
(A) RP	27.6	<1E–03	–2.03	<1E–03	2.11	<1E–03	–0.90	0.45
(B) CF _i	–	–	2.26	<1E–03	7.15	<1E–03	–3.73	0.10
(C) Binder level	–0.58	0.89	–0.87	0.02	9.22	<1E–03	–11.08	0.01
(D) Disintegrant level	1.17	0.82	0.09	0.85	–3.62	0.02	3.82	0.42
(E) Binder source	–2.30	0.29	6.02E–04	1.00	–0.71	0.24	–0.92	0.64
(F) Lubricant type	–7.59	0.001	–0.23	0.23	–0.38	0.52	–2.34	0.23

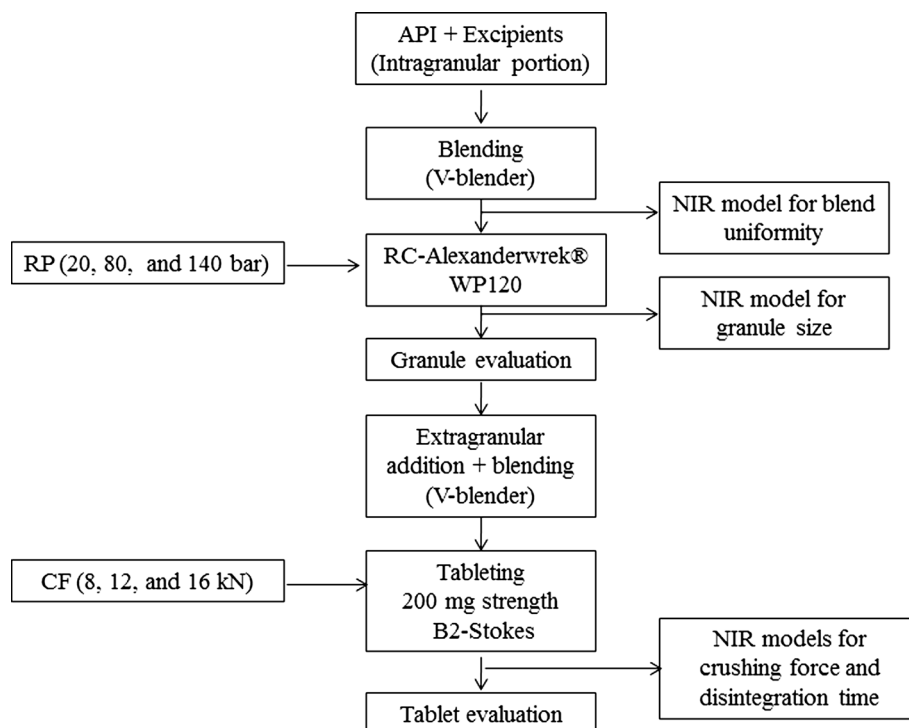


Fig. 3. Process flow chart for ciprofloxacin hydrochloride immediate release tablets

approximately 2 g samples were collected from three different regions (Fig. 4) of the V-blender using powder sampling thief (model no. 5200, Conbar, Monroeville, NJ) and the blend uniformity model was used to determine the uniformity of subsequent formulation blends. The concentration of CIP was determined as described below.

Ciprofloxacin HCl Assay

The amount of CIP was analyzed using high-performance liquid chromatography (HPLC). Mobile phase consists of 0.025 M phosphoric acid (adjusted to pH 3.0±0.1 with triethylamine): acetonitrile (87:13, v/v). The assay was validated, and the assay acceptance criteria included $R^2 > 0.995$ for

each calibration curve, at least six calibrators passing accuracy where a calibrator passes accuracy if percent accuracy <15% and QC samples showing percent accuracy <15%. For tablet analysis, the tablets were crushed and diluted in mobile phase to a concentration of 0.2 mg/mL. The solution was sonicated for 20 min and filtered through 0.45 µm polyethersulfone membrane filters (Millipore, MA). Then 10 µL of this solution (0.2 mg/mL mobile phase) was injected into HPLC (Waters® Corporation, Milford, MA) equipped with an Inertsil® ODS 3 C-18 Column (GL Sciences, Torrance, CA) at a flow rate 1.5 mL/min, and the amount of CIP was determined at 278 nm. For dissolution studies, the samples collected were filtered using 0.45 µm syringe filters and injected into chromatographic system and the amount of CIP was analyzed as described above.

Table IV. Component and Compositions Used for Blend Uniformity Study

Ingredients	Amount (%; w/w)								
	1	2	3	4	5	6	7	8	9
Ciprofloxacin HCl	45	48	50	52	53	54	55	58	61
MCC (Avicel® PH-102)	47	44	42	41	39	37	36	34	31
Hydroxypropyl cellulose	2	2	2	2	2	2	2	2	2
Starch® 1500	5	5	5	5	5	5	5	5	5
Magnesium stearate	1	1	1	1	1	1	1	1	1

Formulation 5 represents center point of batches

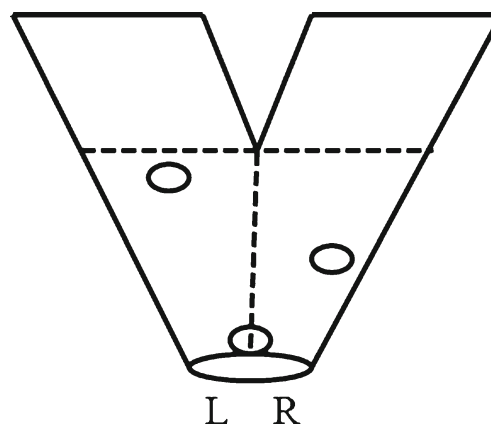


Fig. 4. V-blender showing sampling locations

Tablet Manufacturing

The blends were compressed into 200 mg strength CIP tablets fitted with 11.11 mm (7/16 in.) biconcave tooling on an instrumented Stoke B2 rotary press (Key Industries, NJ) rotating at 30 rpm. The compression force was monitored using an instrumented eye bolt connected to a four channel isolation amplifier (NI-SCXI-1121) and signal conditioning chassis (NI-SCXI-1000) manufactured by National Instruments Corporation (Austin, TX). Signals were monitored using a Labview software (version 8.20) data acquisition system. An identical rotary press using the same processing conditions was employed to manufacture tablets from the granules obtained from 2nd manufacturing site.

Characterization of Granules and Tablets

The granules were characterized for granule size (X), bulk density (Db), tapped density (Dt), and Carr's index (CI %). Tablets were characterized for CF, DT, weight variation (Wt), and dissolution (Q30). Particle size was measured by laser diffraction method using Malvern® Mastersizer (Malvern Inc., Worcestershire, UK); to calculate the particle size, the Fraunhofer model analysis routine in the Malvern instrument software was used. The dry powder feeder was operated at air pressure of 20 psi at a constant feed rate of 2.5 and samples size of 5 g. The reported volume mean granule diameter $D[4,3]$ and span $(D_{90}-D_{10}) / D_{50}$ are the average of three runs. Dbs were determined using USP 26 method <616> Db and Dt of Powders, Method II; the tester was obtained from Sargent-Welch (VWR® Scientific Products), and Dts were determined using JEL Stampf® Volumeter Model STAV 2003 (Ludwigshafen, Germany) in accordance with USP 26 general chapter <616>. *In vitro* dissolution studies were evaluated using USP method II. The dissolution media consists of 0.01 N HCl, the paddles were operated at 50 rpm, and the temperature was maintained at $37 \pm 0.5^\circ\text{C}$. The concentration of CIP was measured using UV-visible spectroscopy model Spectronic® Genesis™ (Thermo Scientific, Pittsburgh, PA) at 276 nm wavelength. Tolerance limits are NTL 80% released in 30 min. Disintegration was performed used basket-rack assembly (USP 26 general chapter <701>). Water was used as media and the temperature was maintained $37 \pm 0.5^\circ\text{C}$. Six tablets were used and time to completely disintegrate was recorded. Tablet CF was determined using hardness tester (Model HT-300) manufactured by Key International, Inc. (Englishtown, NJ).

NIR Multivariate Calibration Model Development

Prior to calibration model development, PCA was performed on the spectra to study the relationship between variables. An appropriate preprocessing method was applied to the spectra to improve model fit. Samples selection was performed to detect spectral outliers and redundant samples based on Mahalanobis distance in the principal component space, which relates the distance of a spectrum from the center of the distribution of spectra. A variety of math pretreatments such as baseline correction (BC), Savitsky-Golay (SG), 2nd derivative (2D; order 2; window 10), normalization (NM) (1-Norm, area=1), and standard normal variate (SNV) were tried to find the method that gave the best model fit. The best

pretreatment was selected based on the method that yielded lowest statistical errors (SEC and SECV). To validate the calibration model, the cross-validation was performed using Vision® software; the algorithm was a variation of the leave-one-out method in which a subset of the samples were selected by the software, for the studies a subset of samples was chosen (segment size=10) and using this algorithm the SEC or SECV were calculated. The prediction residual error-sum squares (PRESS) plot was used to help determine the optimum number of factors for a model. After PCA, PLS models were developed; the details of these models are given below.

Blend Uniformity Model

The neat spectra of CIP and the other excipients were overlaid, see Fig. 5a, and examined, and it was found that in the region 1,600–1,700 nm CIP had a characteristic peak and the excipients in the formulation had minimal absorbance. Spectra from 27 scans (nine concentrations in triplicates; Table IV) were scanned, and the spectral region 1,500–1,700 nm was used for model development. The spectra were preprocessed using SG followed by 2D, and four factors were selected. The model was validated using independent samples selected by the software that were not used in the calibration models; for external calibration, 23 independent validation samples were taken from the site 2 blend samples that were also assayed using HPLC, see Table II. To test for bias, the predicted data was compared with HPLC data to test for accuracy (Table V).

Granule Size Model

Granules obtained from different roll presses were first examined using PCA. For the PCA model, 42 samples were preprocessed using SG followed by 2D and Autoscale, see Fig. 6a. From Table II and Fig. 5b, it was evident that increasing the RP increased the granule size and increased the granule's NIR absorption. For PLS model development, 17 samples from different RPs from batch 1–14 (see Table II) were used for model development. Spectra were preprocessed using SG and 2D. Volume mean granule size was used $D(4,3)$ for the constituent values. Vision® Software randomly selected samples from the calibration to perform internal cross-validation. The model was validated using 14 samples, 1 from the 14 different batches. The validated model was used to predict granule size from site 1, and data was compared with Malvern data, showing no statistical difference. When model was applied to granules obtained at site 2, it did not predict well, *i.e.*, SEP values were unacceptably large.

Crushing Force Model

Similar to granules size model, the first step was to examine the spectra; 54 samples (Fig. 6b) obtained at different RP and compression forces were used. For PCA, preprocessing included NM, SG, 2D, and auto-scaling. As described earlier, batches 1–14 was each compressed at three different compression force (8, 12, and 16) kN force leading to a total of 42 different lots. Three tablets from each lot ($42 \times 3 = 126$) were used for model development. The 126 tables had consisting of different Klucel and MgSt source and different RPs were

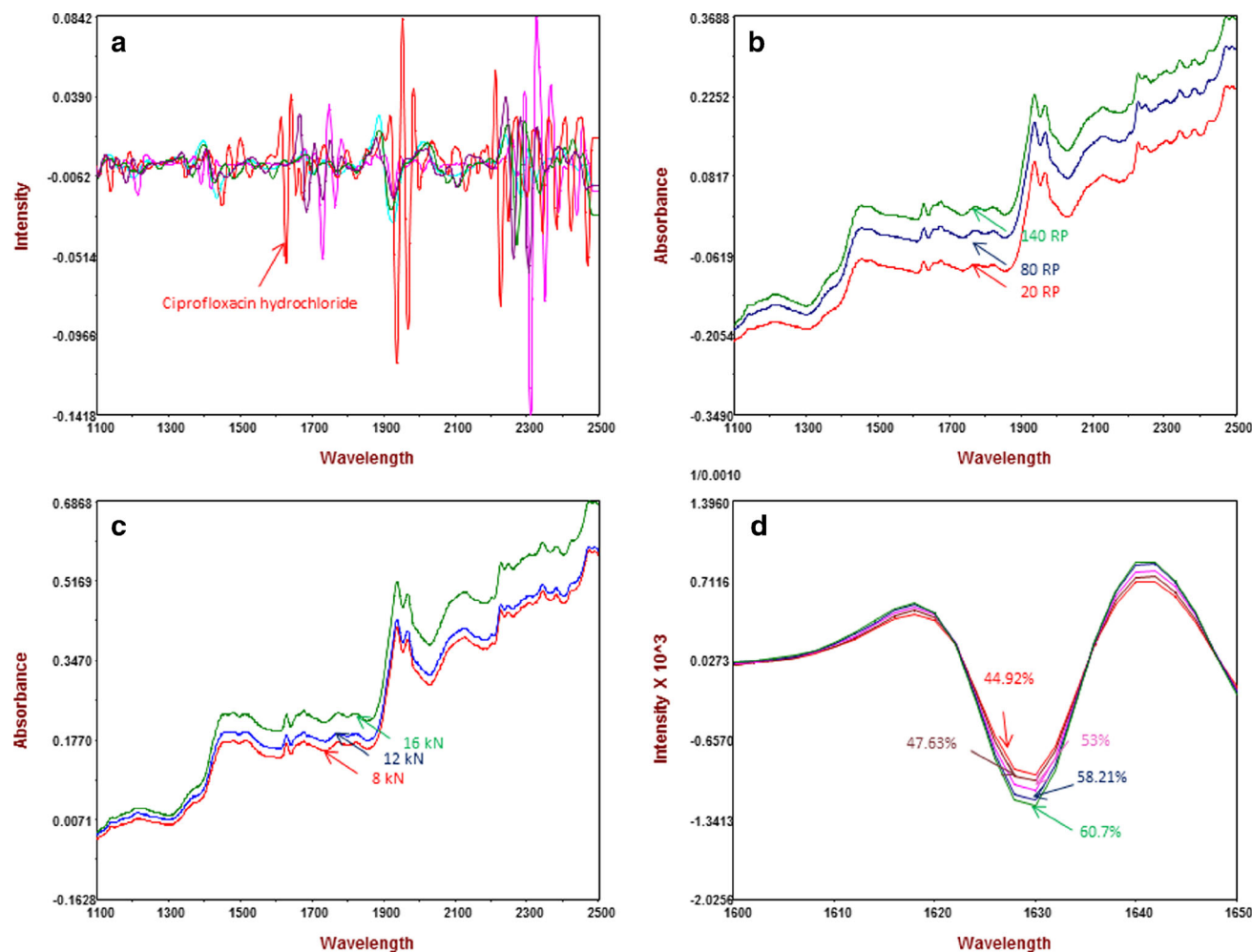


Fig. 5. Feasibility study, 2nd derivative spectra of neat ciprofloxacin hydrochloride and all the excipients given in Table I (a). Overlaid raw spectra of granules (b) obtained at different roll pressures (Table II, batches 1–3) and overlaid raw spectra of tablets obtained at different compression force (Table II, batch 1) (c). The 2nd derivative spectra of blends used to construct blend uniformity calibration model (Table IV, batches 1, 2, 5, 8, and 9) (d)

preprocessed using SG smoothing and BC ($\lambda=1,800$ nm). The entire spectrum was used for calibration model development, and six factors were chosen based on the SEC, SECV, and PRESS values. The calibration model was validated using 84 tablets, where two tablets from each batch and not used in model development were randomly chosen by the software from each of the 42 lots. The validated model did a good job predicting the CF of tablets from site 1, as indicated by a comparison of the SEP and CF was comparable to actual data. However, when applied to site 2 tablets, high SPE was obtained.

Disintegration Time Model

Similar to CF model, 126 samples from 42 lots was used for model development. The entire wavelength range was used to build the model. The spectra was pretreatment included SG smoothing and BC ($\lambda=1,800$ nm). The model was validated using 42 samples, *i.e.*, one tablet from 42 lots from site 1 resulting in good SEP values. However, high SEP was obtained similar to the CF model.

RESULTS AND DISCUSSION

Granule Properties

The summary of the granule and tablet characteristics are presented in Table II. Batches 1–14 were manufactured at site 1 and batches 15–25 were manufactured site 2. Granules obtained from site 1 were compressed at three CF_T, 8, 12, and 16 kN resulting in 42 lots. Granules from site 2 were all compressed at 12 kN, except for batch 23, which was compressed at 16 kN resulting in 11 lots.

A first order regression model was developed using batches 1–14, for each of the granule and tablet quality attributes studied in the form shown below.

$$Y_i = b_0 + b_1A + b_2B + b_3C \dots + b_6F \quad (1)$$

Y_i , response (D[3,4], CF, DT, or Q30); b_0 , intercept; b_1 – b_6 , regression coefficients; A , linear effect of RP; B , linear effect of CF; C , linear effect of binder level; D , linear effect

Table V. NIR Spectroscopy and HPLC Results for Testing the Accuracy

Blends	Accuracy		
	NIR (%; w/w)	HPLC (%; w/w)	Residual
1	53.20	49.93	3.27
2	54.79	52.29	2.50
3	52.56	51.46	1.10
4	53.28	52.65	0.63
5	53.54	50.72	2.82
6	52.66	51.49	1.17
7	53.02	51.64	1.38
8	52.75	51.01	1.74
9	51.49	52.49	-1.00
10	53.73	53.18	0.55
11	54.00	52.15	1.85
12	51.72	51.22	0.50
13	52.46	51.91	0.55
14	53.10	52.96	0.14
15	47.62	50.30	-2.68
16	49.84	52.80	-2.96
17	49.20	51.30	-2.10
18	48.21	51.30	-3.09
19	51.06	51.60	-0.54
20	49.52	53.50	-3.98
21	49.58	51.10	-1.52
22	49.64	50.90	-1.26
23	49.43	48.50	0.93
Average	51.58	51.58	0.00
Standard deviation	2.04	1.14	2.01
<i>t</i> test	0.49		

of disintegrant level; *E*, linear effect of binder source; and *F*, linear effect of lubricant type.

Regression analysis (Table III) indicates that RP had a significant influence ($p=0.0001$) on the granule size followed by the type of lubricant used ($p=0.0011$). Increasing RP from 20 to 140 bars increased the average granule size; this was accompanied by the decrease in relative span (spread of granule size distribution). It is well known that increasing in RP produces ribbons with higher tensile strength due to higher degree of material consolidation in the nip region (23); when these ribbons were milled, the granule size was larger compared with ribbons produced at a lower RP. Granule size increased when MgSt-M was replaced with MgSt-D (Table III). This behavior can be explained by differences in the particle size and surface area of monohydrate (10.6 μm) and dihydrate forms (14.3 μm) as reported by Okoye *et al.* (24). Batches 1, 12, 3, and 13 from site 1 (Table II) and 15, 19, 20, and 22 from site 2 have the same formulation composition and were processed under same RP conditions. This data clearly indicates that the granules size obtained at two manufacturing sites were statistically different; this occurred despite our best efforts to keep the experimental conditions the same at both sites. Given the fact that the formulations and materials used at both sites were the same, a possible reason for this difference could be due to the fact that even though all the settings were identical; there could be calibration differences; thus, the actual parameters were different. However, without verifying all the operating parameters it will be impossible to determine if this was the reason for these differences.

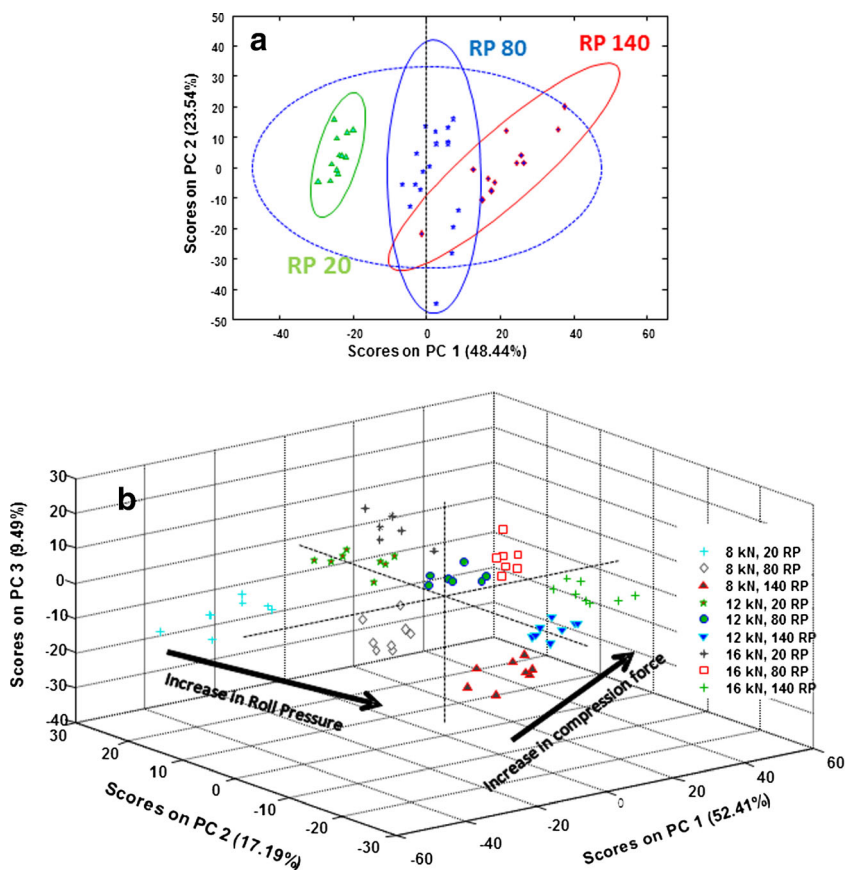


Fig. 6. PCA score plots for granules (a) and tablets (b). The spectra were preprocessed using 2nd derivative followed by autoscale

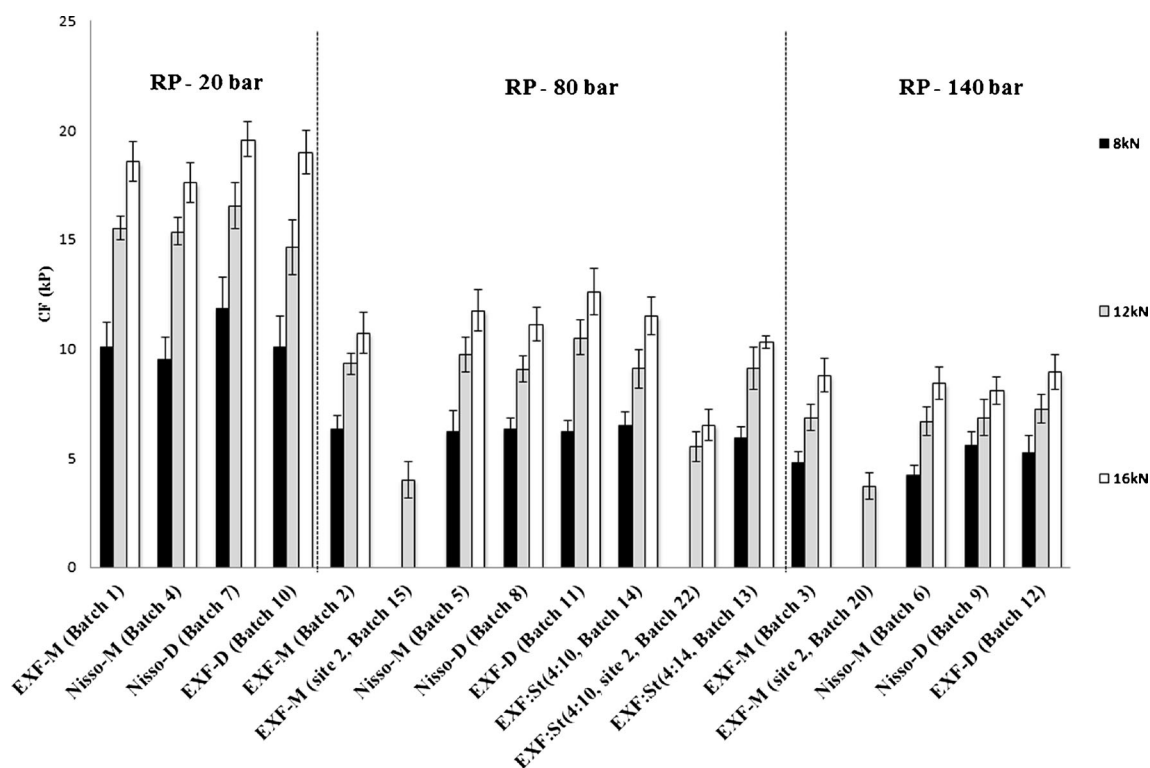


Fig. 7. Influence of roll pressures and compression force on the crushing force. Batch composition with Klucel® EXF and MgSt-M as EXF-M, Nisso-L and MgSt-M as Nisso-M, Nisso-L and MgSt-D as Nisso-D, and Klucel® EXF and MgSt-D as EXF-D. Batches manufactured at second site are denoted as site 2. Batches with different binder (*EXF*) and starch® 1500 levels are presented as EXF-St

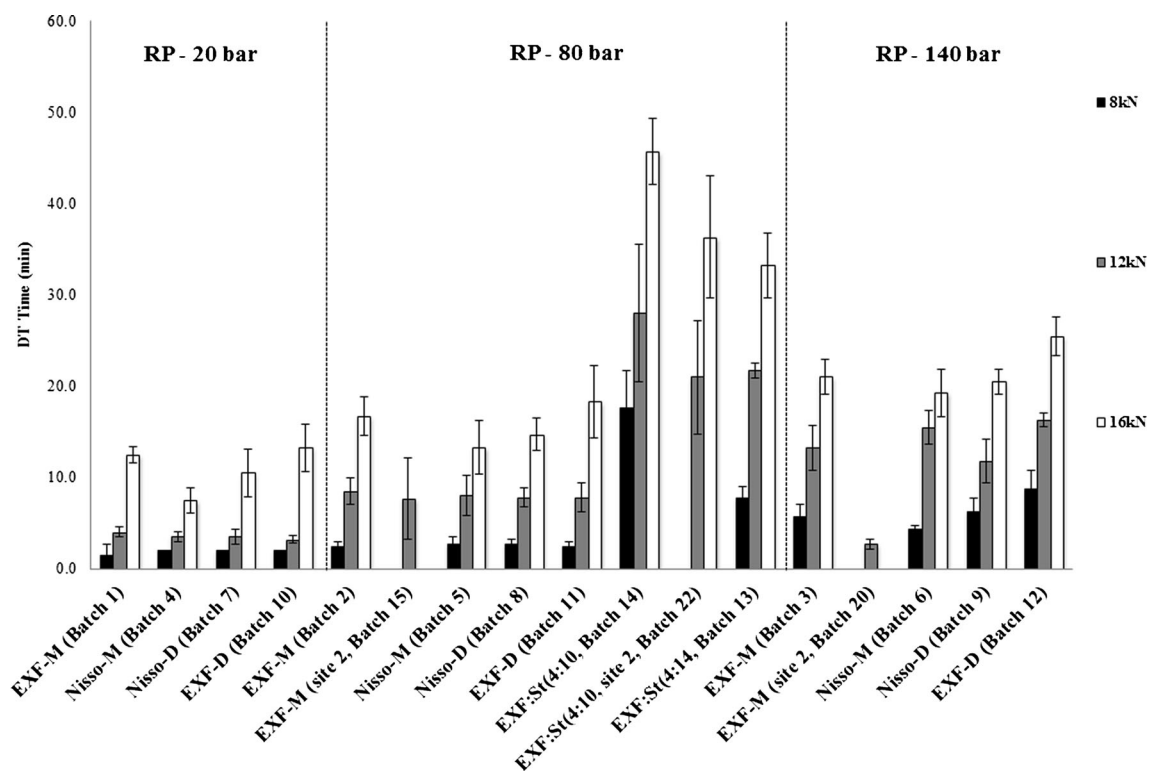


Fig. 8. Influence of roll pressures and compression force on the disintegration time. Batch composition with Klucel® EXF and MgSt-M as EXF-M, Nisso-L and MgSt-M as Nisso-M, Nisso-L and MgSt-D as Nisso-D, and Klucel® EXF and MgSt-D as EXF-D. Batches manufactured at second site are denoted as site 2. Batches with different binder (*EXF*) and starch® 1500 levels are presented as EXF-St

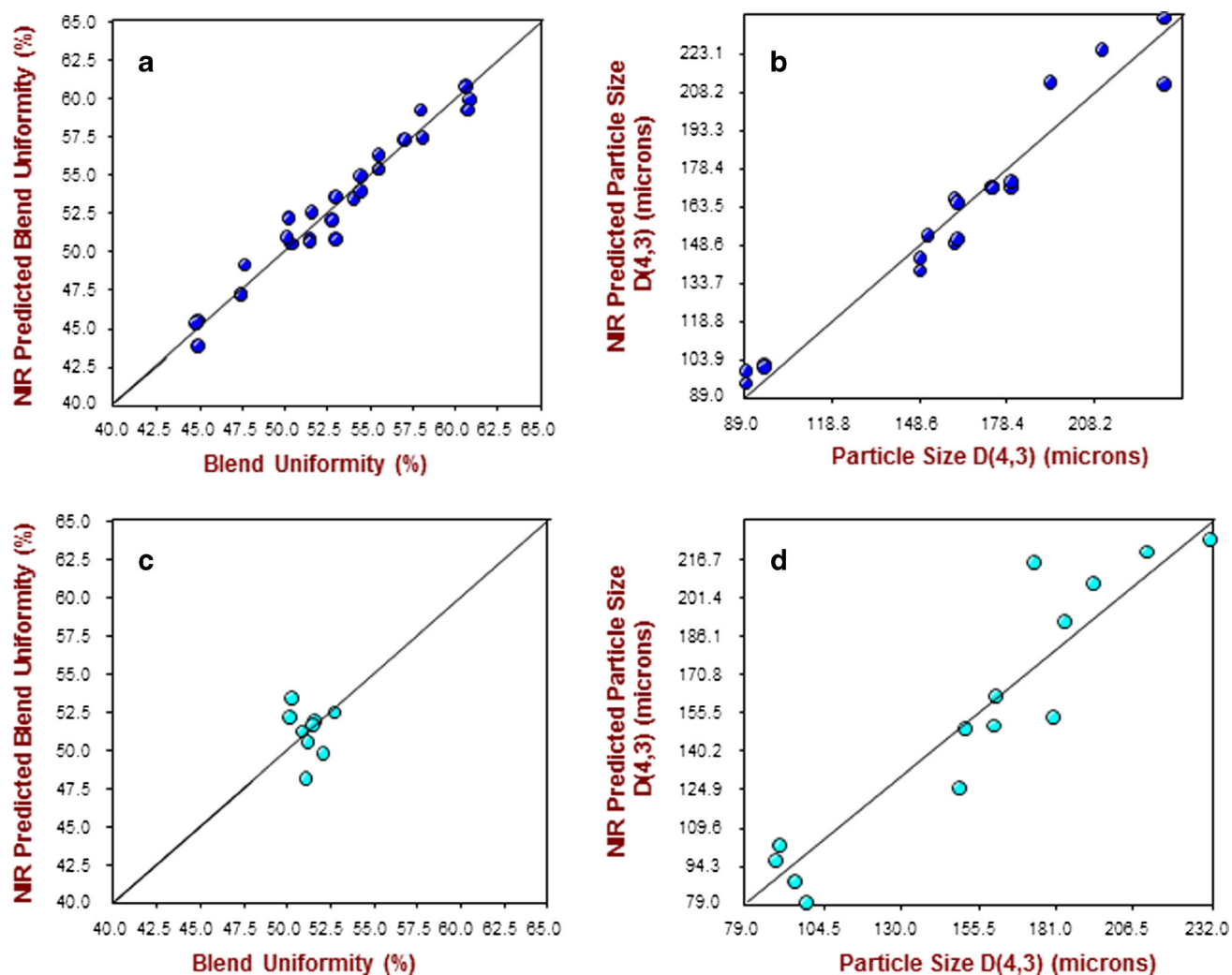


Fig. 9. PLS calibration models for blend uniformity (a), granule size (b). PLS prediction (validation) for blend uniformity (c) and granule size (d)

Tablet Properties

The influence of processing parameters and formulation treatments on the CF is presented in Fig. 7. Increasing the RP at a given compression force decreases the CF of the tablets. This can be explained by loss of compactability or work-hardening phenomenon commonly observed with plastic materials such as MCC. Several authors have reported that this work-hardening phenomenon results in a pronounced decreased in tensile strength (2,3,23,25,26). In addition, for a given RP, an

increase in compression force increased the CF of the tablets. It was also observed that increase in the HPC binder level from 2% to 4% significantly increase the CF of the tablets. To identify significant parameters, linear regression was performed and a $p < 0.05$ is considered significant. A summary of regression coefficients and p values is in Table III. For CIP release; RP, compression force, binder levels and disintegrant levels were found to be statistically significant for the DT (Fig. 8), whereas, the amount of binder used was the only significant factor for CIP release after 30 min (Q30).

Table VI. Summary of PLS Models for the Granule and Tablet Quality Attributes

Models	Calibration model						Prediction model—site 1		Prediction model—site 2	
	No. of samples	Preprocessing method	No. of factors	R^2	SEC	SECV	No. of samples	SEP	No. of samples	SEP
Blend uniformity	27	SG quadratic 2D	4	0.961	1.03	2.14	—	—	23	1.79
Granule size	17	SG quadratic 2D	4	0.949	11.16	15.50	14	18.42	—	—
Crushing force	126	BC, SG quadratic 2D	6	0.849	1.71	1.99	88	2.21	27	2.23
Disintegration time	126	BC, SG quadratic 2D	6	0.886	3.47	4.38	42	4.51	30	10.32

Factors such as the binder type ($p=0.64$; Klucel® EXF vs Nisso®-L) and magnesium stearate type ($p=0.23$; MgSt-D vs MgSt-M) were insignificant for the CF and the CIP release profile.

The granules manufactured at site 2 were compressed into tablets using an identical rotary press under same operating conditions. CF (Fig. 7) and disintegration data (Fig. 8) were found to be statistically different from the tablets obtained from site 1. This could be explained due their differences in the granules size which influence the compressibility of the material (3).

NIR Feasibility Study

The 2D overlaid spectra of excipients and neat CIP powder were examined to identify the unique spectral characteristics of the API (Fig. 5a). Characteristic peaks were found at 1,480, 1,504, 1,604, 1,652, 1,912, 2,104, and 2,204. In this study, spectral region 1,600–1,700 nm was selected to construct PLS blend uniformity model, where the CIP spectrum predominates and where there are minimal overlapping spectral peaks from the excipients. The raw NIR spectra of the granules obtained at different RPs (20, 80, and 140 bar) were overlaid

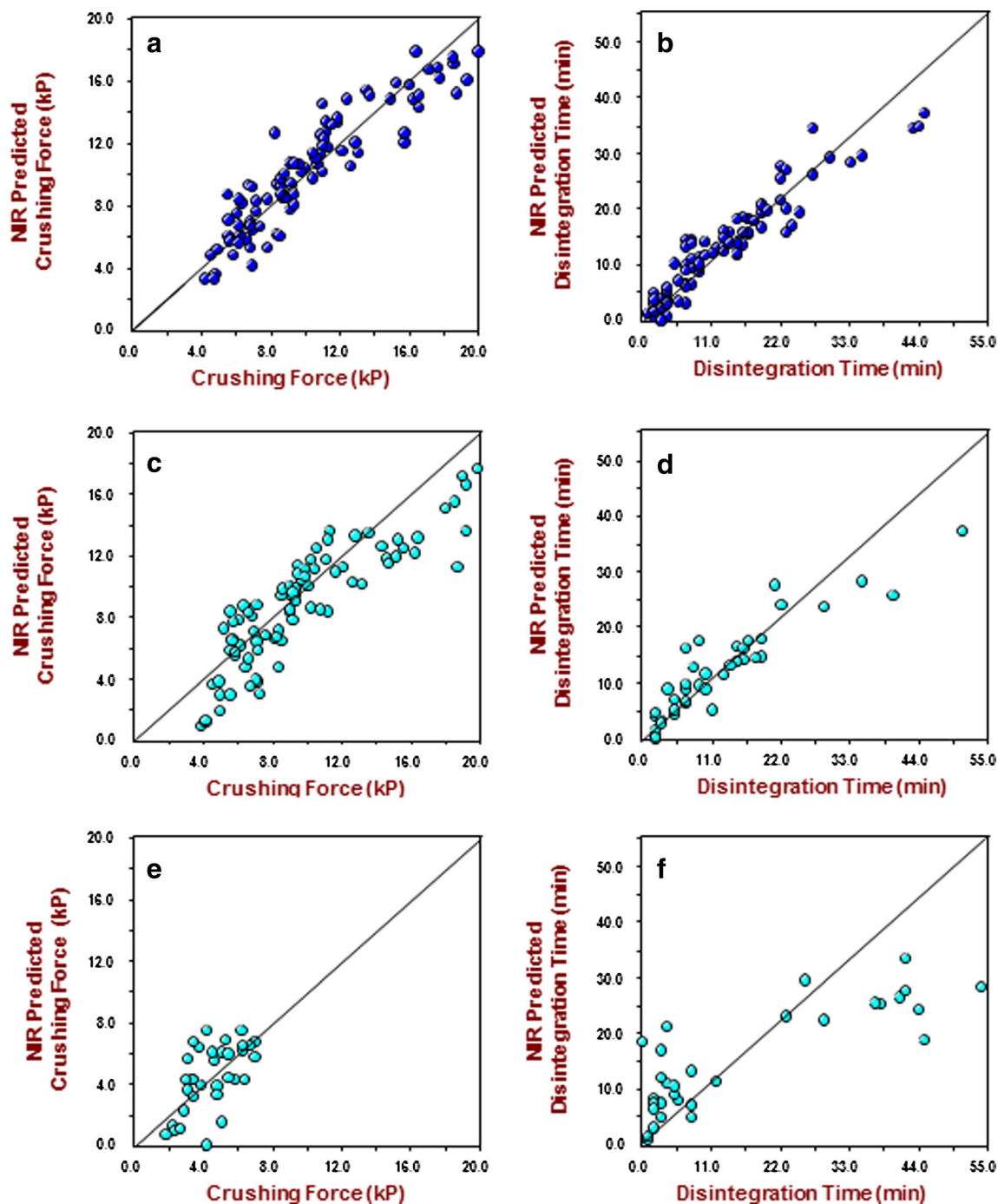


Fig. 10. PLS calibration models for tablets. Crushing force (a) and disintegration time (b). PLS prediction using internal validation set crushing force (c) and disintegration time (d) and external validation crushing force (e) and disintegration time (f)

and the spectra were analyzed for variations, a non linear baseline shift was observed; this may be due to increase in the density of the granules with higher RP (Fig. 5b). Similar baseline shift was observed when the raw spectra of the tablets produced at different tablet compression forces (8, 12, and 16 kN) were examined; it was reported that increase in tablet compression force increased the tablet density which affected its absorbance *via* changes in the diffused reflectance path length (Fig. 5c) (9,11–13). Figure 5d is the 2D overlaid spectra of CIP. As the amount of CIP increases in the blend matrix, the intensity of the peaks increased.

Prior to the calibration model development, PCA was performed on the samples. A total of 54 tablets was selected from nine different lots (batches 1–3, Table II) processed at different RC pressures (20, 80, and 140 bars) and compressed at three different compression force (8, 12, and 16 kN). The 3D PCA score plot results (Fig. 6b) indicate that three PCs contained 79.1% of the total variability in the dataset (PC1, 52.4%; PC2, 17.2%; and PC3, 9.5%). Examination of the score plot indicated that PC1 correlated with tablet compression force and PC2 explained samples differences due to RP; a detailed discussion of this data is in the modeling sections below. The sample variation could be explained by differences in the densities arising from increased compression force during tableting and increased RP during RC.

Blend Uniformity Model

Figure 5d shows the spectral regions 1,600–1,700 nm used for the blend uniformity, which has a CIP characteristic peak. For the calibration model development, the samples were preprocessed using SG (quadratic polynomial, no of convolutions=7) followed by 2D (segment size=10) using 1,500–1,700 nm spectral region. Four factors were used to build the model, and R^2 , SEC, and SECV obtained were 0.961,

1.03%, and 2.14%, respectively (Fig. 9a). The model when tested with external dataset resulted in SEP values of 1.79% (Fig. 9c). To assess model fit, we examined the measured vs predicted R^2 , SEC, SECV, and SEP, see Table VI; in addition, to test for model accuracy, paired t test was performed on the NIR predicted and HPLC data. Results indicate no significant difference ($p=0.49$) between the data (Table V).

Granule Size Model

The spectra of granules obtained at different RPs were subjected to PCA to identify the relationships among the variables. The raw spectrum was preprocessed using 2D followed by auto-scaling. The PCA 2D plot of 42 samples (Fig. 6a) accounts for 78.1% of the total variability in the spectra. PC1 had 48.1% of the total variability, and this variability correlated with the RP used to make the ribbon. To build a calibration model for the average particle size $D(4,3)$, which was measured using the Malvern Mastersizer, was used for the regression constitutive values. A four-factor PLS calibration model was obtained when samples were pretreated with SG (cubic polynomial, 29 convolutions) and 2D using 1,128–2,170 nm spectra regions. The model (Fig. 9b) resulted in R^2 , SEC, and SECV values of 0.949, 11.1 μm , and 15.4 μm , respectively. The model was validated using external dataset using the granules not used in the model from the same roller compactor, *i.e.*, no site change and the resulting prediction model (Fig. 9d) resulted in SEP value of 18.4 μm . Adjusting bias did not significantly improve the model indicating the robustness of the model. There was no statistical significance difference ($p>0.05$) between the NIR predicted data and the actual granule size measured using laser diffraction.

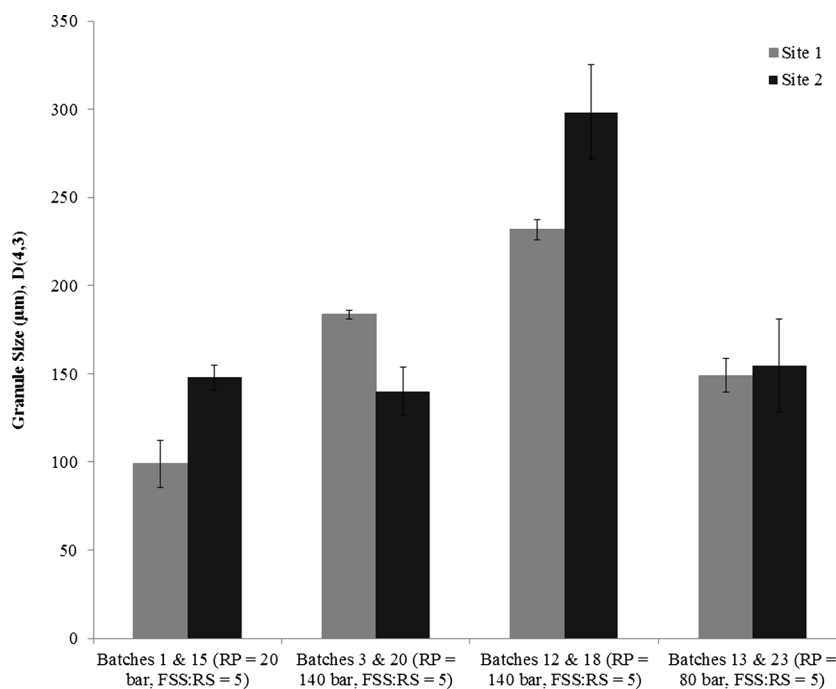


Fig. 11. Particle size comparison for batches process under similar roller compaction parameters and similar formulation manufactured at different sites

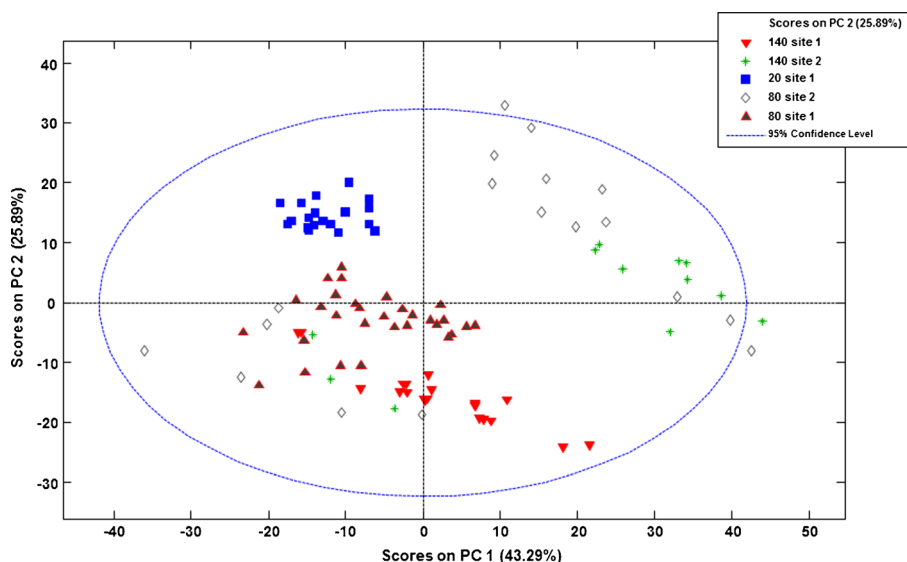


Fig. 12. PCA analysis and score plots of granules obtained at different roll pressure and compression force

Crushing Force Model

For the CF calibration model development, 126 tablets were selected from batches 1–14 with different excipient grades, varying formulations as well as roller compacted processing parameters. For this study, PLS model provides the best fit and the final pretreated selected was SG smoothing (quadratic polynomial, seven convolutions) and BC ($\lambda=1,800$ nm). The calibration model (Fig. 10a) was built using six factors with R^2 , SEC, and SECV of 0.849, 1.7, and 2.0 kp, respectively, using 1,122–2,192 nm spectra regions. The models developed were tested using validation batches obtained from the same roller compactor and tablet press not used in the calibration model consisting of 88 samples. The results (Fig. 10c) had a correlation SEP value of 2.2 kp, adjusting the bias did not change the SEP value indicating the robustness of the calibration model. Statistical analysis using student t test indicate no significant difference ($p>0.05$) between NIR predicted values (mean= 9.74 ± 4.11 kp) and actual data (mean= 9.74 ± 3.79 kp). However, the prediction values

(Fig. 10e) for the batches manufactured at site 2 resulted in higher SEP values for the batches with similar formulation and manufacturing conditions.

Disintegration Time Model

For this study, 126 samples were selected from batches 1–12 to build calibration model; these batches for the calibration dataset consisted of tablets made from different Klucel® (EXF or Nisso-L) and magnesium stearate (MgSt-M or MgSt-D) source only. Sample selection was performed using Mahalanobis distance in the principal component space (threshold 0.95). The best-fit model was obtained when SG 1,122–2,192 nm wavelength range was used. The samples were pretreated using BC ($\lambda=1,800$ nm) and SG smoothing. The calibration model (Fig. 10b) gave R^2 value of 0.886 when six factors were used to build the model and SEC and SECV of 3.5 and 4.4 min, respectively. The final model was tested using prediction set consisting of 42-sample set from four different batches resulting in a SEP value of 4.5 min (Fig. 10d). Similar to CF results, DT prediction values (Fig. 10f) for the batches

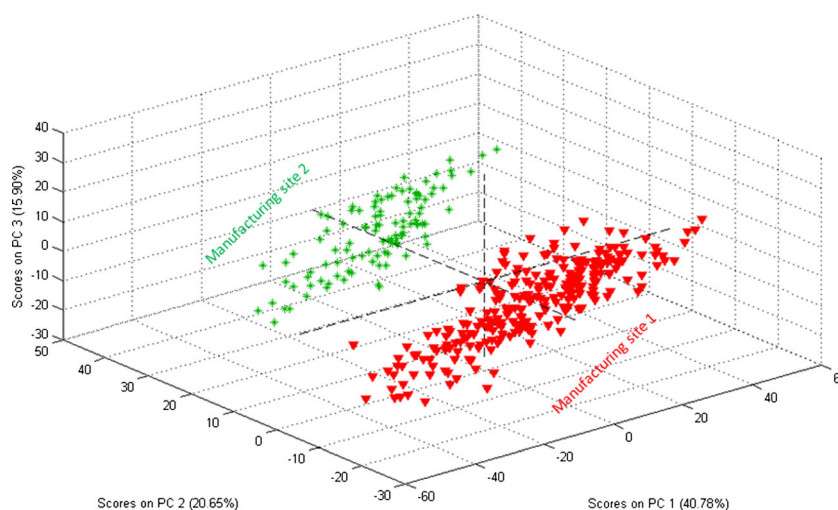


Fig. 13. PCA analysis and score plots of tablets obtained at different manufacturing sites

manufacture site 2 was found to be higher. The results of which are further discussed below.

Model Prediction Using External Dataset (Manufacturing Site 2)

To test model validity on an external dataset, calibration models were applied to external batches that were manufactured at the 2nd location using the same model roller compactor that was run with identical process settings as the first roller compactor. The granules and tablets obtained at the different site were evaluated for granule size, CF, and DT, and results show that the granules were different from calibration dataset (Table II). Figure 11 shows the granule sizes obtained at the different sites as measured using Malvern Mastersizer. The batches with the same formulations, materials and processing parameters made on the 2nd roller compactor had subtly but statistically significant different particle sizes from site 1 particles, as shown in Fig. 11. The resulting granules were compressed on a tablet press and the compression profile was monitored using a force transducer. The granules from site 2, led to downstream quality changes such as different CFs and DTs; this was despite the fact that the tablet press use to compress both sets of granules was identical. The prediction summary is presented in the Table V. It was evident that the models (Fig. 10e, f) did not result in satisfactory SEP values for the CF and DT. This means that the unknown processing differences at site 2 lead that resulted in different granule and tablet character were not incorporated in NIR models. To describe this variability, PCA was performed on both the granules and on tablets obtained from both manufacturing sites (Figs. 11 and 12). PC-1 (43.2%) in Fig. 12 and PC-2 (20.7%) in Fig. 13 clearly shows the spectral variation resulting from granules and tablets used in the calibration and validation set, respectively.

CONCLUSIONS

This study demonstrates the application of NIR spectroscopy as a powerful tool to monitor CQAs such as blend uniformity, granule size, tablet CF, and DT during the formulation development of immediate release tablets. As a part III of a three-part study, the PLS multivariate models were developed, validated and applied during the production. The models were able to successfully predict the CQAs for the granules and tablets manufactured in the same site and on same machine. However, the standard error of prediction values (SEP) were found to be higher when applied to granules manufactured at a different locations, which emphasizes the importance of incorporating all the variability that may arise due to process and/or instrument variability. In addition, PCA was able to clearly demonstrate their difference and was used a qualitative tool in the manufacturing.

ACKNOWLEDGMENTS

The authors would like to acknowledge the financial assistance from the FDA and CIPET. Drs. Bancha Chuasuwan, Ramesh Dandu, and Walter Xie for their technical assistance with the CIP assay. Thanks to Ryan McCann for his assistance with roller compaction at Purdue University, School of Pharmacy.

Disclaimer The views expressed in this manuscript are the personal opinion of the authors and do not necessarily reflect the views or policies of the FDA

Glossary

ANOVA	Analysis of variance
CF _t	Compression force
D or D(3,4)	Volume mean diameter
DT	Disintegration time
D _t	Tapped density
D _b	Bulk density
NIRS	Near-infrared spectrometry
PAT	Process analytical technology
PCA	Principal component analysis
PCR	Principal component regression
PLS	Partial least squares
PLSR	Partial least square regression
PRESS	Prediction residual error-sum squares
SEC	Standard error of calibration
SECV	Standard error of cross-validation
SEP	Standard error of prediction
SG	Savitzky–Golay
2nd D	Second derivative

REFERENCES

1. Teng Y, Qiu Z, Wen H. Systematical approach of formulation and process development using roller compaction. *Eur J Pharm Biopharm.* 2009;73(2):219–29.
2. Malkowska S, Khan KA. Effect of re-compression on the properties of tablets prepared by dry granulation. *Drug Dev Ind Pharm.* 1983;9(3):331–47.
3. Sun C, Himmelspach M. Reduced tabletability of roller compacted granules as a result of granule size enlargement. *J Pharm Sci.* 2006;95(1):200–6.
4. Roberts RJ, Rowe RC. The effect of punch velocity on the compaction of a variety of materials. *J Pharm Pharmacol.* 1985;37(6):377–84.
5. Ruegger CE, Celik M. The effect of compression and decompression speed on the mechanical strength of compacts. *Pharm Dev Technol.* 2000;5(4):485–94.
6. Bacher C, Olsen PM, Bertelsen P, Kristensen J, Sonnergaard JM. Improving the compaction properties of roller compacted calcium carbonate. *Int J Pharm.* 2007;342(1–2):115–23.
7. Inghelbrecht S, Remon JP. Roller compaction and tableting of microcrystalline cellulose/drug mixtures. *Int J Pharm.* 1998;161(2):215–24.
8. Daugherty PD, Chu JH. Investigation of serrated roll surface differences on ribbon thickness during roller compaction. *Pharm Dev Technol.* 2007;12(6):603–8.
9. Tabasi S, Fahmy R, Bensley D, O'Brien C, Hoag S. Quality by design, part I: application of NIR spectroscopy to monitor tablet manufacturing process. *J Pharm Sci.* 2008;97(9):4040–51.
10. ICH. Q8(R2): Pharmaceutical development. Part I: pharmaceutical development, and part II: annex to pharmaceutical development. http://www.ich.org/fileadmin/Public_Web_Site/ICH_Products/Guidelines/Quality/Q8_R1/Step4/Q8_R2_Guideline.pdf (2009).
11. Cantor S, Hoag S, Ellison C, Khan M, Lyon R. NIR spectroscopy applications in the development of a compacted multiparticulate system for modified release. *AAPS PharmSciTech.* 2011;12(1):262–78.
12. Tabasi S, Fahmy R, Bensley D, O'Brien C, Hoag S. Quality by design, part II: application of NIR spectroscopy to monitor the coating process for a pharmaceutical sustained release product. *J Pharm Sci.* 2008;97(9):4052–66.
13. Tatavarti A, Fahmy R, Wu H, Hussain A, Marnane W, Bensley D, *et al.* Assessment of NIR spectroscopy for

- nondestructive analysis of physical and chemical attributes of sulfamethazine bolus dosage forms. *AAPS PharmSciTech*. 2005;6(1):E91–9.
14. Gupta A, Peck G, Miller R, Morris K. Influence of ambient moisture on the compaction behavior of microcrystalline cellulose powder undergoing uni-axial compression and roller-compaction: a comparative study using near-infrared spectroscopy. *J Pharm Sci*. 2005;94(10):2301–13.
 15. Gupta A, Peck G, Miller R, Morris K. Real-time near-infrared monitoring of content uniformity, moisture content, compact density, tensile strength, and Young's modulus of roller compacted powder blends. *J Pharm Sci*. 2005;94(7):1589–97.
 16. Soh J, Boersen N, Carvajal T, Morris K, Peck G, Pinal R. Importance of raw material attributes for modeling ribbon and granule properties in roller compaction: multivariate analysis on roll gap and NIR spectral slope as process critical control parameters. *J Pharm Innov*. 2007;2:106–24.
 17. ICH: Q9 Quality Risk Management. http://www.ich.org/fileadmin/Public_Web_Site/ICH_Products/Guidelines/Quality/Q9/Step4/Q9_Guideline.pdf (2005).
 18. ICH: Q10 Pharmaceutical Quality System. http://www.ich.org/fileadmin/Public_Web_Site/ICH_Products/Guidelines/Quality/Q10/Step4/Q10_Guideline.pdf (2008).
 19. Fahmy R, Kona R, Dandu R, Xie W, Claycamp G, Hoag S. Quality by design I: application of failure mode effect analysis (FMEA) and Plackett-Burman design of experiments in the identification of “main factors” in the formulation and process design space for roller-compacted ciprofloxacin hydrochloride immediate-release tablets. *AAPS PharmSciTech*. 2012;13(4):1243–54.
 20. Claycamp G, Kona R, Fahmy R, Polli J, Martinez M, Hoag S. Quality-by-design II: application of quantitative risk analysis to the formulation of ciprofloxacin tablets. in preparation for *PharmSciTech*. 2012.
 21. Desai D, Rinaldi F, Kothari S, Paruchuri S, Li D, Lai M, *et al.* Effect of hydroxypropyl cellulose (HPC) on dissolution rate of hydrochlorothiazide tablets. *Int J Pharm*. 2006;308(1–2):40–5.
 22. Olivera ME, Manzo RH, Junginger HE, Midha KK, Shah VP, Stavchansky S, *et al.* Biowaiver monographs for immediate release solid oral dosage forms: Ciprofloxacin hydrochloride. *J Pharm Sci*. 2011;100(1):22–33.
 23. Lim H, Dave V, Kidder L, Neil Lewis E, Fahmy R, Hoag S. Assessment of the critical factors affecting the porosity of roller compacted ribbons and the feasibility of using NIR chemical imaging to evaluate the porosity distribution. *Int J Pharm*. 2011;410(1–2):1–8.
 24. Okoye P. Lubrication of direct-compressible blends. *Pharm Technol*. 2007;31(9):116.
 25. Dave V, Fahmy R, Bensley D, Hoag S. Eudragit® RS PO/RL PO as rate-controlling matrix-formers via roller compaction: influence of formulation and process variables on functional attributes of granules and tablets. *Drug Dev Ind Pharm*. 2012.
 26. Dave V, Fahmy R, Hoag SW. Roller Compaction of Eudragit polymers Part 2. *Drug Dev Ind Pharm*. 2011; Submitted to *Drug Dev Ind Pharm*.